JOURNAL OF OPTOELECTRONICS AND ADVANCED MATERIALS, Vol. 10, No. 9, September 2008, p. 2390 – 2395

Gas sensing properties of samarium substituted lithium ferrite

C. DOROFTEI[a,b*], E. REZLESCU[b], N. REZLESCU[b], P.D. POPA[b]
[a]*University" Al. I. Cuza " , B-dul Carol I , 11 , 700506, Iasi, Romania*
[b]*Institute of Technical Physics, B-dul D. Mangeron 47, 700050 Iasi, Romania*

Microstructure and gas sensitivity of pure and samarium substituted lithium ferrites, $Li_{0.5}Sm_xFe_{2.5-x}O_4$ (x = 0, 0.05, 0.1 and 0.2), prepared by sol-gel-selfcombustion were studied. As test gases acetone, ethanol, methanol, LPG, butane and ammonia were used. By SEM investigation was evidenced that Sm ions induced microstructural changes in Li ferrite. The finest granulation (bellow 100 nm) and highest porosity (44%) were observed in $Li_{0.5}Sm_{0.2}Fe_{2.3}O_4$. The sensitivity measurements evidenced that the gas sensitivity depends on the working temperature and gas type. All ferrites are sensitive to acetone, ethanol and methanol and less sensitive to ammonia, LPG and butane. The best sensitivities, over 85%, were obtained at operating temperatures of 340 – 355^{0}C for ethanol, methanol and acetone.

(Received February 16, 2008; accepted August 14, 2008)

Keywords: Ferrites, Substitutes, Structure, Gas sensitivity

1. Introduction

The first decade of the 21 century has been labeled by some as the "Sensor Decade". There is an increasing interest in the finding new materials in order to develop high performance solid-state gas sensors. Gas sensors are important in environmental monitoring, home safety and chemical controlling.

Many different semiconducting oxides in bulk ceramic [1, 2], thick film [3] and thin film [4, 5] have been studied as candidate sensor element for gas sensing.

Spinel-type oxide semiconductors are an alternative for no expensive and robust detection systems because of good chemical and thermal stability under the operating conditions [6-9]. The sensing mechanism consists in the change of the electrical resistivity resulting from chemical reaction between gas molecules and the metal oxide surface [10, 11].

The surface morphology has an essential role on the sensitivity of solid state sensors. The nanograined materials offer new opportunities for enhancing the performance of gas sensor because of their high surface to volume ratio [12-15]. For these reasons, the researches try new routes to prepare semiconductor materials. In this paper sol-gel-selfcombustion method was applied to prepare nanostructured lithium based ferrites. The rapid heating and cooling during self combustion reaction can produce materials with high specific surface area which is beneficial for gas detection.

Li ferrite behaves as a n-type semiconductor based on the inverse spinel structure being characterized by high electrical resistivity (10^5 – 10^6 Ω·cm) and high Curie temperature (640 – 680^{0}C) [16].

The present paper reports the results concerning microstructural characterization of $Li_{0.5}Fe_{2.5-x}Sm_xO_4$ (x = 0, 0.5, 0.1 and 0.2) ferrites, the effect of `rare earth (Sm) substituent on the electrical properties and on the gas sensing characteristics. The gas sensing characteristics were obtained by measuring the sensitivity as a function of various factors like Sm concentration, operating temperature, type and concentration of the test gas and, finally, the response time.

It was evidenced that all ferrites are sensitive to acetone, ethanol and methanol and less sensitive to ammonia, butane and liquefied petroleum gas (LPG).

2. Experimental

Powders of $Li_{0.5}Sm_xFe_{2.5-x}O_4$ (x = 0, 0.05, 0.1 and 0.2) ferrites were prepared by sol-gel-selfcombustion method which includes:

- solution of metal nitrates [$Fe(NO_3)_3 \cdot 9H_2O$, $LiNO_3$, $Sm(NO_3)_3$] in deionized water;
- polyvinyl alcohol addition to first solution to make colloidal solution;
- NH_4OH addition to increase pH to about 8;
- stirring at 80^{0}C;
- drying at 120^{0}C of the gel;
- finally, selfcombustion.

The combusted powders were calcined at 500^{0}C for 30 minutes to remove the residual organic compounds. The calcined powders were subjected to cold uniaxial pressing followed sintering in air for 2 hours at 850^{0}C of the compressed pellets. The detailed step by step procedure has been reported in [17].

The morphology has been analyzed by scanning electron microscope (TESLA BS 340). The size of the ferrite crystallites was determined from SEM micrographs by linear intercept method [18]. For electrical measurements, sintered pellets were silvered on a flat surface as in Fig.1. The silver electrodes were heat treated at 500^0C for 2 minutes to evaporate the dextrine from the silver paste.

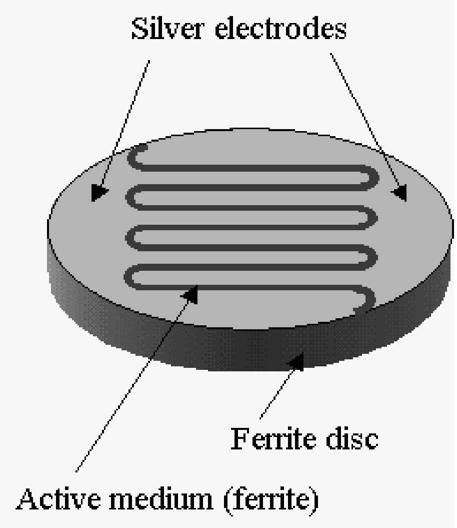

Fig.1 Design of ferrite sensor with silver electrodes

To evaluate gas sensing properties the silvered platelet was placed on a heater, inside a glass enclosure; its resistance in air was measured with a digital LCR meter at 10 Hz. For sensitivity measurements, the test gases (ethanol, methanol, acetone, ammonia, butane and LPG) were injected with a syringe into the glass chamber and the resistance was measured in the presence of test gas (air + test gas) at fixed operating temperatures, from 100^0C to 390^0C, both in the presence of test gas (R_g) and in air (R_a). A cromel-alumel thermocouple located in close proximity of the platelet measures the temperature. After each experiment, the resistivity of the sample in air was measured again.

The sensitivity S was calculated as the ratio:

$$S = \frac{\Delta R}{R_a} = \frac{R_a - R_g}{R_a} \qquad (1)$$

All data were collected after gas exposure for 15 - 20 minutes. After each change of the test gas, the sensor element was activated by its submitting to heat cleaning at 500^0C for 5 minutes.

3. Results and discussion

3.1. Microstructure

The external morphology of the sintered pellets can be visualized from the scanning electron micrographs given in Fig.2. In the undoped sample (Fig.2a) one can observe the presence of macro-agglomerations, of about 2 μm in size. Within the macro-agglomerations the particle sizes are small, under 200 nm. Many large pores are located at the junction of the agglomerates. A radical change in the microstructure can be observed when Sm is incorporated. The size of the agglomerations decreases and many dispersed mini-agglomerations appear. A slight decrease in the grain size, from 0.2 μm to 0.1 – 0.15 μm and an increase in the porosity, from33.2% to about 44%, were obtained (Table 1), when Sm substitution increased, from x = 0 to x = 0.2. The surface specific area for compounds was found to be between 10.4 m^2/g for pure ferrite and 22 m^2/g for $Li_{0.5}Fe_{2.3}Sm_{0.2}O_4$ (Table 1). The lower surface area for pure ferrite is due to the presence of large and dense aggregates (hard agglomerates). Also, the porosity increases by Sm incorporation (Fig.2 b, d). The increase in porosity cannot be caused by material evaporation during the heat treatment at 850^0C. The weight loss ($\Delta m/m_0$) was evaluated to be very small, between 0.08% and 0.24 % (Table 1).

Table 1. Some properties of $Li_{0.5}Sm_xFe_{2.5-x}O_4$ (x = 0, 0.05, 0.1 and 0.2) ferrites sintered at 850^0C for 2 hours

Symbol	Chemical formula	Density d (g/cm^3)	Porosity p (%)	Weight loss (%)	Average particle size D_m (nm)	Specific surface area A_{sp} (m^2/g)	Activation energy E_a (eV)	Resistivity at room temperature ρ_{RT} (Ω·cm)
L1	$Li_{0.5}Fe_{2.5}O_4$	2.88	33.24	0.246	200	10.4	0.67	$1.15\cdot10^9$
L2	$Li_{0.5}Sm_{0.05}Fe_{2.45}O_4$	2.85	35.03	0.169	180	11.7	0.53	$1.33\cdot10^9$
L3	$Li_{0.5}Sm_{0.1}Fe_{2.4}O_4$	2.74	36.63	0.080	150	14.6	0.50	$9.58\cdot10^8$
L4	$Li_{0.5}Sm_{0.2}Fe_{2.3}O_4$	2.72	44.23	0.126	100	22.0	0.71	$5.90\cdot10^8$

One can remark from Fig. 2 that the open porosity predominates. However, in the Sm containing ferrites there is a substantial amount of closed porosity which hinders the densification during the sintering process. Some properties of the ferrite pellets are summarized in Table 1. The surface area, A_{sp}, was calculated with formula [19]:

$$A_{sp} = \frac{S}{Vd} = \frac{6}{dD_m}, \qquad (2)$$

were S and V are the surface area and volume of the ferrite particle, D_m is the average particle size and d is the bulk density.

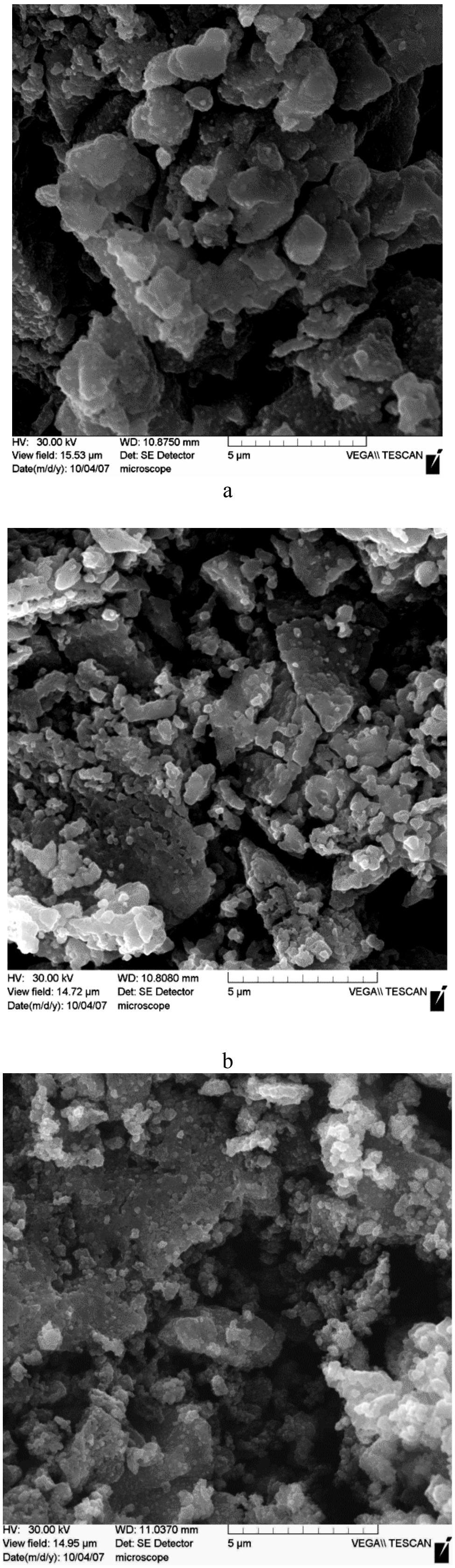

a

b

c

Fig. 2.SEM micrographs for: a) $Li_{0.5}Fe_{2.5}O_4$; b) $Li_{0.5}Sm_{0.1}Fe_{2.4}O_4$; c) $Li_{0.5}Sm_{0.2}Fe_{2.3}O_4$.

3.2. Electrical and gas sensing properties

The electrical conduction in Li-ferrite is attributed to electron hopping between the two valence state of iron, Fe^{2+} and Fe^{3+} on the octahedral sites in the spinel lattice [16].

The Fe^{2+} ion concentration depends upon several factors such as sintering temperature, atmosphere, and grain structure. In Li ferrite it is possible that some amount of Fe^{2+} ions appears due to Li evaporation during the heat treatment. But, this possibility can be excluded because the mass loss measured after heat treatment at 850^0C was very small, bellow 0.25%. The room temperature resistivity for all samples is given in Table 1. It is noted that the values of the resistivity ($10^8 - 10^9$) are higher than those reported for Li ferrite prepared by ceramic method [20]. This discrepancy may be understood from the following two aspects. One aspect is the nanograined structure obtained by sol-gel-selfcombustion route. Small crystallite sizes imply an increase of the insulating surface on the grain boundaries which normally accounts for high electrical resistance of the polycrystalline material. The other aspect is that the porous structure of these samples impedes the motion of charge carriers leading to an increase of the resistivity. The less lower values of resistivity in the samples L3 and L4 may be due to the valence fluctuations between Sm^{3+} and Sm^{2+} ions localized on the octahedral sites.

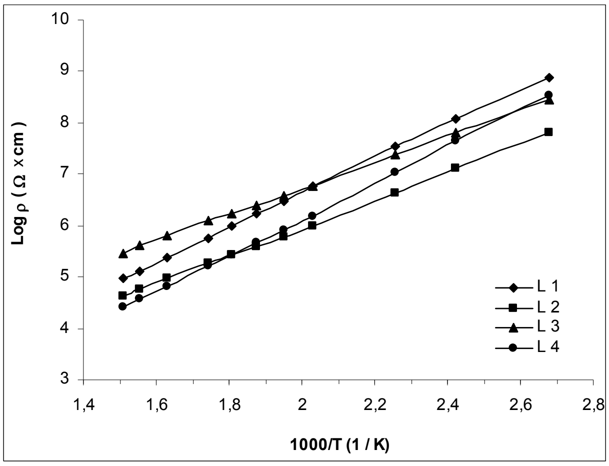

Fig.3. Dependence log ρ versus 1/T for Li0.5SmxFe2.5$_{-x}$O$_4$: L1 (x = 0); L2 (x = 0.05); L3 (x = 0.1); L4 (x = 0.2).

From the almost linear dependence log ρ vs. 1/T (Fig. 3) the E_a values for all samples were calculated. The high E_a values (0.5 – 0.7 eV) (Table 1) are compatible with the high resistivity values.

In regard to gas sensing properties, the sensitivity of the electrical resistivity to acetone, ethanol, methanol, LPG, butane and ammonia was investigated in the temperature interval 100 – 390^0C. It is known that the gas-sensor element reaction typically occurs at elevated temperatures (150 – 600^0C) [11, 21].

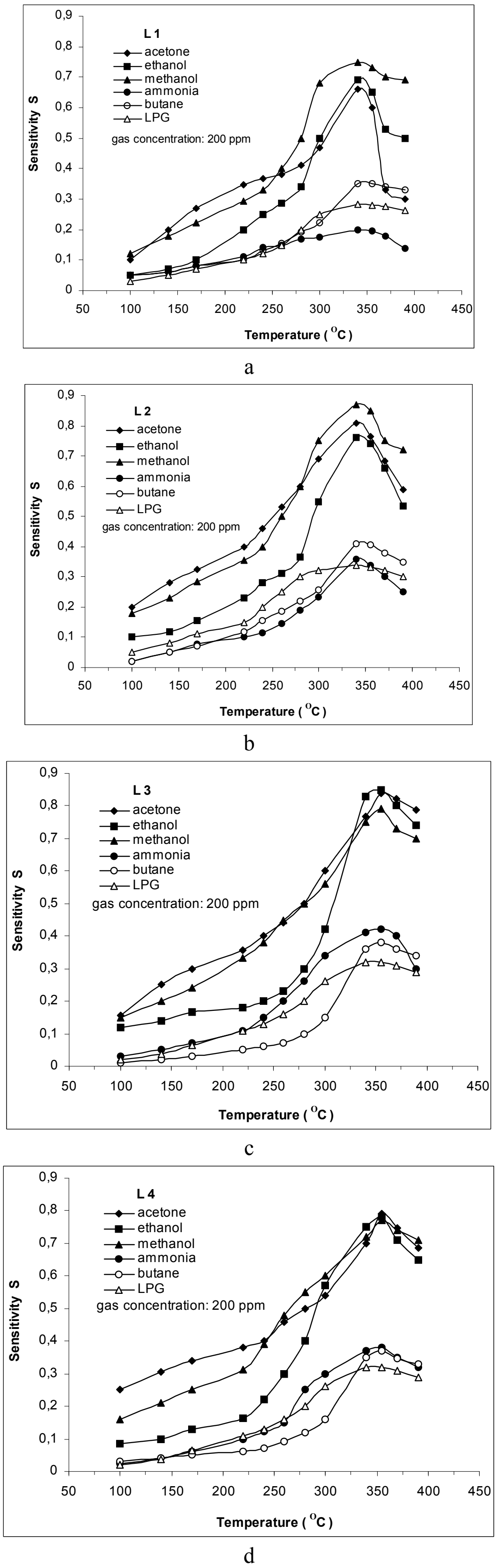

a

b

c

d

Fig. 4 Gas sensitivity versus operating temperature for: $Li_{0.5}Fe_{2.5}O_4$ (L1); $Li_{0.5}Sm_{0.05}Fe_{2.45}O_4$ (L2); $Li_{0.5}Sm_{0.1}Fe_{2.4}O_4$ (L3); $Li_{0.5}Sm_{0.2}Fe_{2.3}O_4$ (L4)

Fig.4 (a – d) shows the sensitivity characteristics of the pure and samarium substituted lithium ferrites versus working temperature. Some observations can be made:

- The gas sensitivity increases with increasing temperature and reaches a maximum value at optimum temperature which is of 340^0C for L1 and L2 samples and of 355^0C for L3 and L4 samples.
- An interesting result is that the gas sensitivity of the ferrites strongly depends on the detected gas type. The sensitivity to acetone, ethanol and methanol (85% – 87%) is higher than to butane, LPG or ammonia (bellow 40%).
- The pure Li ferrite is less sensitive than Sm containing ferrites.

In Fig.5 are compared the sensitivities of all samples at optimum temperature, towards test gases.

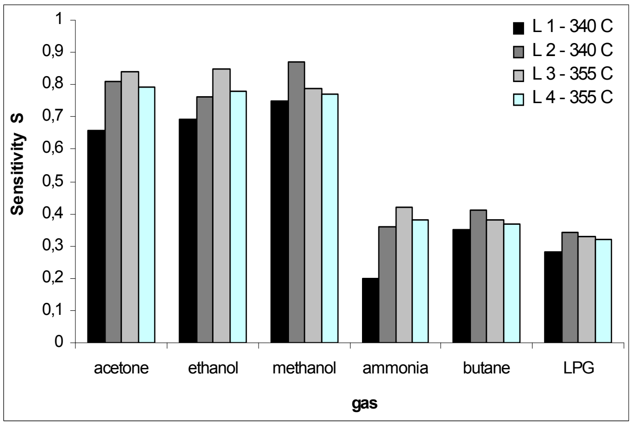

Fig. 5. Bar diagram for sensitivities to test gases of $Li_{0.5}Sm_xFe_{2.5-x}O_4$: L1 (x = 0), L2 (x = 0.05), L3 (x = 0.1) and L4 (x = 0.2) at optimum temperature.

A number of experiments have been carried out around the optimized temperature and all the time the sensitivities of the samples are the same, indicating the reliability of the sensor for long life.

The improved sensitivity towards ethanol or methanol can be explained by the involvement of the hydroxyl group OH^-. When the ferrite sensor is in the presence of the ethanol or methanol vapor, the OH^- group reacts with oxygen on the sensor surface, generating free electrons by which conductivity increases [5]. The possible reaction between ethanol and ionic oxygen is the following [22, 23]

$$CH_3CH_2OH + 6\ O^- \rightarrow 2\ CO_2 + 3\ H_2O + 6\ e^- .$$

We mention that all sensitivity measurements presented in this paper were collected at least 15 – 20 minutes after the gas exposure to make steady the resistance. This presumably is the minimum time for the gas molecules to diffuse through the compressed ferrite powder. This time required to reach steady conditions does not change at different temperatures, which suggest that the gas diffusion into the porous sample is not critically dependent on the working temperature, but on the porosity within the ferrite.

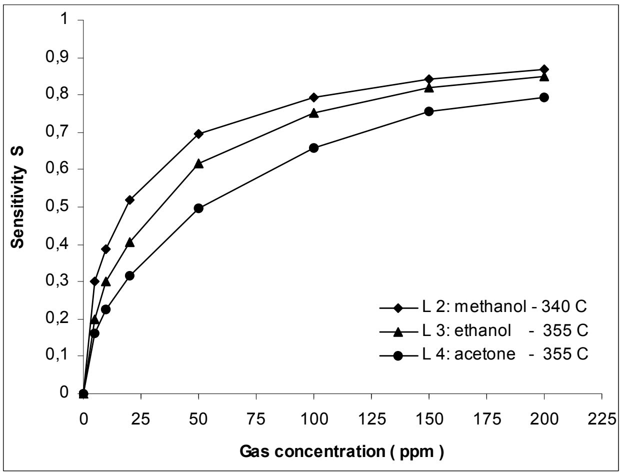

Fig. 6. Gas sensitivity versus gas concentration of samarium substituted Li-ferrites: L2 (x = 0.05), L3 (x = 0.1) and L4 (x = 0.2)

Fig. 6 plots the variation of gas sensitivity of Sm containing Li ferrites as a function of stepwise increasing gas concentration. Measurements were made at optimum working temperature, by injecting various amounts of ethanol, methanol or acetone into the sealed chamber to increase the gas concentration from zero to 200 ppm. The sensitivity significantly increases with increasing the gas concentration up to 100 ppm and then, this tends to a saturation value. For example, the measured sensitivities for L2 sample ($Li_{0.5}Fe_{2.45}Sm_{0.05}O_4$ composition which has the best sensitivity to methanol) were around 52%, 70%, 80% and 86% as the methanol concentrations were 25, 50, 100 and 200 ppm respectively.

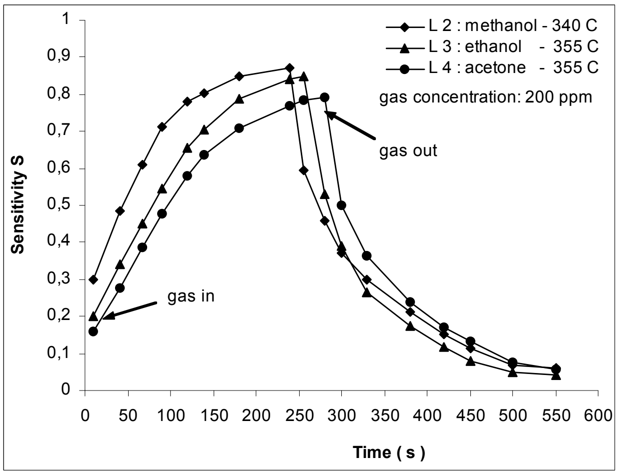

Fig. 7. Response characteristics to methanol, ethanol and acetone for samarium substituted ferrites: L2 (x = 0.05), L3 (x = 0.1) and L4 (x = 0.2), at optimum temperatures of 340^0C and 355^0C.

Another important factor for every gas sensor is the response and recovery time, when the sensor is exposed to and then removed from a gas. Some response characteristics to methanol, ethanol and acetone (200 ppm) of Sm substituted ferrites are given in Fig.6. One can see that the elements quickly responded when the test gas was injected. The response time required for the sensitivity attains 90% of its maximum value is shorter (of about 2 minutes) for L2 ferrite (x = 0.05) than that of L3(x = 0.1) and L4 (x = 0.2) ferrites. The time taken by the sensor element to come back once the test gas was removed is found to be longer, of about 3 – 4 minutes.

4. Conclusions

The obtained results in the present work show that samarium substituted lithium ferrite, prepared by sol-gel-selfcombustion route are suitable for ethanol, methanol or acetone sensing applications. In the case of 200 ppm gas concentration and 340 – 355^0C temperature, the response time is of about 2 minutes for a sensitivity of 80% – 87%. $Li_{0.5}Sm_{0.05}Fe_{2.45}O_4$ is more sensitive to methanol (87% sensitivity), $Li_{0.5}Sm_{0.1}Fe_{2.4}O_4$ can be used for ethanol and acetone sensing (85% sensitivity) and **Li0.5Sm0.1Fe2.4O4** has the same sensitivity (80%) to acetone, ethanol and methanol.

The obtained results incite to deeper investigations on the gas sensors based on nanostructured Li ferrites.

References

[1] M. Aslam, V. A. Chaudhary, I. S. Mulla, S. R. Sainkar, A.B. Mandale, A. A. Belhekar, K. Vijayamohanan, Sensors and Actuators B Chemical **75**, 162 (1999).
[2] N. Rezlescu, C. Doroftei, E. Rezlescu, P. D. Popa, Physica Status Solidi A **203,** 306 (2006).
[3] D. R. Patil, L. A. Patil, G. H. Jain, M. S. Wagh, S.A. Patil, Sensors & Transducers Journal **74**, 874 (2006).
[4] Z. Jin, H. J. Zhou, Z. L. Jin, R. F. Savinell, C. C. Liu, Sensors and Actuators B Chemical **52**, 188 (1998).
[5] I. Ferreira, R. Igreja, E. Fortunato, R. Martins, Sensors and Actuators B Chemical **103**, 344 (2004).
[6] X. Q. Liu, Z. L. Xu, Y.S. Shen, J. Yunnan Univ. **19**, 147 (1997).
[7] C. V. G. Reddy, S. V. Manorama, V. J. Rao, Sensors and Actuators B **55**, 90 (1999).
[8] N. S. Chen, X. J. Yang, E. S. Liu, J. L. Huang, Sensors and Actuators B **66**, 178 (2000).
[9] N. Rezlescu, C. Doroftei, E. Rezlescu, P. D. Popa, Sensors and Actuators B: Chemical **115**, 589 (2006).
[10] A. Gurlo, N. Barsan, U. Weimar, Mechanism of NO_2 Sensing on SnO_2 and In_2O_3 Thick Film Sensors as Revealed by Simultaneous Consumption and Resistivity Measurements, in The 16th European Conference on Solid-State Transducers, Prague, Czech. Republic, 15-18 September 2002, pp.970-973.

[11] T. G. G. Maffeis, G. T. Owen, M. W. Penny, T. K. H. Starke, S. A. Clark, H. Ferkel, S. P. Wilks, Surface Science **520**, 29 (2002).
[12] R. Rella, P. Siciliano, S. Capone, M. Epifani, L. Vasanelli, A. Liciulli, Sensors and Actuators B **58**, 283 (1999).
[13] M. Ferroni, D. Boscarino, E. Comini, D. Gnani, G. Martinelli, P. Nelli, V. Rigato, G. Sberveglieri, Sensors and Actuators B **58**, 289 (1999).
[14] R. Martins, E. Fortunato, P. Nunes, I. Fereira, A. Marques, Journal of Applied Physics **96**, 1398 (2004).
[15] N. Rezlescu, N. Iftimie, E. Rezlescu, C. Doroftei, P. D. Popa, Sensors and Actuators B **114**, 427 (2006).
[16] J. Smit et H. P. J. Wijn, Les Ferrites, Dunod, Paris (1961).
[17] P. D. Popa, N. Rezlescu, Romanian Reports in Physics **52**, 769 (2000).
[18] M. I. Mendelson, J. Amer. Ceram. Soc. **52**, 443 (1969).
[19] C. Laberty, P. Alphonse, J. J. Demai, C. Sarada, A. Rousset, Mater. Res. Bull. **32**, 249 (1997).
[20] A. M. Ahmed, T. S. Bishay, G. Abdelatif, J. Phys. Chem. Solids **62**, 1039 (2001).
[21] L. Satyanarayana, K. M. Reddy, S. V. Manorama, Sens. Actuators, B, Chem. **89**, 62 (2003).
[22] T. Gao, T. H. Wang, Appl. Phys.A **80**, 1451 (2006).
[23] X. L. Cheng, H. Zao, L. H. Huo, S. Gao, J. G. Zhao, Sensors and Actuators B Chemical **102**, 248 (2004).

---

[*] Corresponding author: docorneliu@yahoo.com